Journal of Alloys and Compounds 501 (2010) L33–L37

Contents lists available at ScienceDirect

Journal of Alloys and Compounds

journal homepage: www.elsevier.com/locate/jallcom

Letter

Effects of magnetic field on hydrothermal growth of Cu–Ni system

Mingzai Wu [a,b,*], Xianzhen Du [a], Xianghua Lu [a], Yongqing Ma [a], Xiansong Liu [a], Qingqing Fang [a], Lide Zhang [b]

[a] Key Laboratory of Opto-electronic Information Acquisition and Manipulation (Anhui University), Ministry of Education, Hefei 230039, People's Republic of China
[b] Key Laboratory of Materials Physics, Institute of Solid State Physics, Chinese Academy of Sciences, Hefei 230031, Anhui, People's Republic of China

ARTICLE INFO

Article history:
Received 5 January 2010
Received in revised form 9 April 2010
Accepted 14 April 2010
Available online 22 April 2010

PACS:
81.10.Aj
74.25.Ha
81.10.Dn

Keywords:
Crystal morphology
Hydrothermal crystal growth
Metals
Magnetic materials

ABSTRACT

The induction effects of applied external magnetic field on the morphology, composition and magnetic properties of copper-nickel system grown with hydrothermal method have been investigated in the presence of polyvinyl pyrrolidone (PVP). The products' phases and morphologies are characterized by X-ray diffractometer (XRD) and field emission scanning electronic microscopy (FESEM). Magnetic measurements reveal that the introduction of magnetic field could lead to the enhancement of magnetic parameters, which implies that the magnetic field could exert influences on the nucleation and domain structure of particles.

1. Introduction

In addition to the role played as an important means for the study of magnetic properties of materials [1,2], magnetic field has been reported to exert much influence on chemical, physical and biological systems based on the so-called radical pair mechanism (RPM) [3,4]. In these years, much effort has been made to understand how magnetic fields influence the growth of crystals and the directed aggregation of nanoparticles. For example, magnetic fields were used to direct the orientation of vanadium pentoxide ribbons [5], the growth of Fe_3O_4 nanowires [6], the assembly of magnetic nanoparticles [7–11], mouse osteoblast cells [12], and the alignment of grains and particles [13,14]. It has been developed as an effective auxiliary preparation method for anisotropy nanomaterials with various applications [15,16]. Despite these achievements, most of these researches were focused on the changes of morphology and magnetic properties of the elemental crystal and magnetic oxide from the point of view of assembly. However, the solution growth of binary alloys in the magnetic field has rarely been reported [8,17].

Nanoscale metal and alloys have shown novel optical, electrical and magnetic properties with respect to their corresponding bulk materials. Cu–Ni transition metal system, for its good corrosion resistance and mechanical properties [18], has been applied in marine petroleum engineering. Recently, Cu–Ni nanomaterials have been reported to possess potential application in small-scale electronic devices as atomic-sized metallic point contacts [19] and magnetoresistant application for its peculiar magnetoresistance behavior (GMR) [20]. Considering the magnetic properties difference between Cu (diamagnetic) and Ni (ferromagnetic), we suppose that the magnetic field may affect the microstructure and composition and consequently affect the magnetic properties of the Cu–Ni binary alloy during its synthesis process. In this paper, we report the magnetic field effects on the Cu–Ni hydrothermal system in terms of products' morphological, composition and magnetic properties changes.

2. Experimental

For the present experiment, all the reagents are analytical grade and used as received. In a typical synthesis, nickel nitrate hexahydrate [$Ni(NO_3)_2{\cdot}6H_2O$,

* Corresponding author at: Key Laboratory of Opto-electronic Information Acquisition and Manipulation (Anhui University), Ministry of Education, Hefei 230039, People's Republic of China. Tel.: +86 551 5107284.
E-mail address: mingzaiwu@gmail.com (M. Wu).

0925-8388/$ – see front matter.
doi:10.1016/j.jallcom.2010.04.098

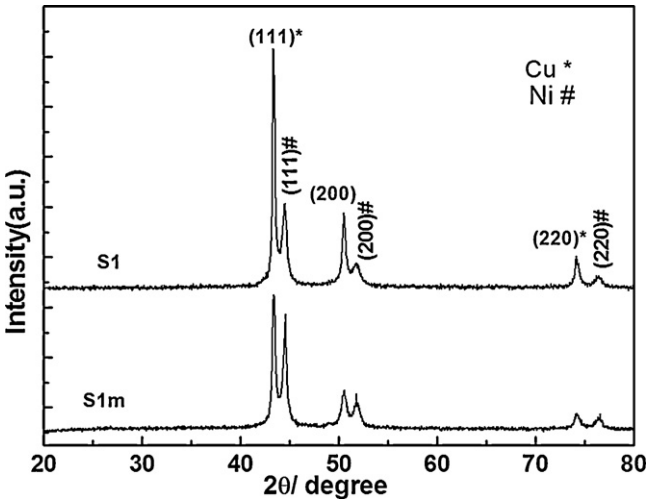

Fig. 1. XRD patterns of samples S1 and S1m. Both of them were indexed as mixtures of Cu and Ni.

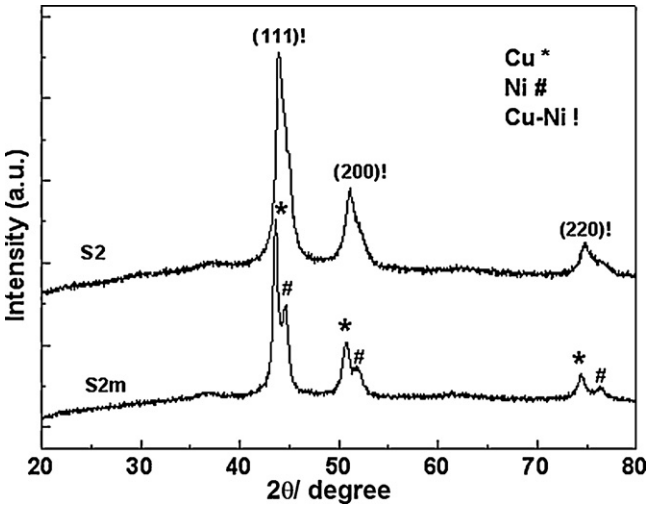

Fig. 2. XRD patterns of samples S2 and S2m.

1.5 mmol], copper chloride [$CuCl_2 \cdot 2H_2O$, 1.5 mmol], PVP [0.3 g] and urea [$CO(NH_2)_2$ 15 mmol] were dissolved in 60 ml Distilled water. After being vigorously stirred for 15 min, 10.0 mL of hydrazine was dropwise added into the above mixture solution. Then the reddish-brown solution was transferred into two Teflon-lined stainless steel autoclaves with 60 ml capacity, respectively (one without external magnetic field, the other with 0.19 T magnet made of NdFeB at 150 °C). Both of the autoclaves were closed tightly to perform hydrothermal processes at 150 °C for 15 h. After the reaction was completed, the resulting black solid powder was washed with alcohol and distilled water three times, respectively. Then the products were dried in air at 50 °C. The as-obtained samples were labeled as S1 and S1m, with m indicating the case of 0.19 T. The same reactions were performed for the case of 1.5 g PVP with other reaction parameters unchanged, which yielded samples S2 and S2m. These as-obtained samples S1, S1m, S2 and S2m were characterized by X-ray powder diffraction (XRD) using an 18 kW advanced X-ray diffractometer with Cu Kα radiation (λ = 1.54056 Å), field emission scanning electron microscope (FESEM, FEI Sirion 200). Magnetic hysteresis loops were measured on a vibrating sample magnetometer (VSM, BHV-55) at room temperature.

3. Result and discussion

In the presence of small dosage of PVP (0.3 g), the phases of the as-obtained sample S1 and S1m are determined by XRD with the patterns shown in Fig. 1. Both of the patterns can be indexed to the mixture of face-centered cubic (FCC) structure of copper (JCPDS 04-0836) and FCC nickel (JCPDS 04-0850). The crystalline size of Ni phase for sample S1 (31 nm) is smaller than that of S1m (43 nm), calculated by Scherrer's equation from the full width at half-maximum of (1 1 1) reflection, which reveals that the application of magnetic field could influence the particles' growth and enhance the crystalline size. Remarkably, the intensity ratio of Ni (1 1 1) peak to Cu (1 1 1) peak becomes larger for the sample prepared with a magnetic field, indicating a preferential orientation of Ni grains in the mixture. These results suggested that the nucleation and growth of crystallites could be influenced by magnetic field.

Fig. 2 shows the XRD patterns of samples S2 and S2m obtained for the case of 1.5 g PVP dosage. Different from S2m, sample S2 possesses the broadened peaks (1 1 1), (2 0 0) and (2 2 0) of the mixture of Cu and Ni and the peak (1 1 1) (43.9°) of sample S2 is located between Cu (1 1 1) (43.3°) and Ni (1 1 1) (44.5°). The reduction of crystalline size should be responsible for the peaks broadening and the location of peak (1 1 1) (43.9°). With the increase of PVP dosage, the adsorption of PVP molecules on the newly formed crystalline seeds would be enhanced, which would hinder the growth of crystalline seeds. The detailed growth mechanism needs further investigation. Interestingly, the application of magnetic field could change the crystalline growth habits and help to index the Ni phase from the mixture of nanocrystalline Cu–Ni mixture in the XRD patterns. In the presence of magnetic field, the free energy of the whole system will be increased by the product of magnetization M and the magnetic intensity H, $-\tilde{M}\tilde{H}$, which would serve as the growth driving force. Considering the ferromagnetism of Ni and diamagnetism of Cu, Ni crystalline seeds would gain free energy $-\tilde{M}_{Ni}\tilde{H}$ in the hydrothermal reduction system, and favor the growth of Ni crystallite. The PVP dosage and the introduction of magnetic field compete with each other for the growth of Ni crystallite in the Cu–Ni composite system.

Fig. 3 further shows the morphological changes effected by the application of magnetic field. Sample S1 is mainly composed of quasi-spherical particles with size distribution around 300 nm, as shown in Fig. 3a; while for S1m, due to the introduction of magnetic field, the Lorentz force would play a role at the level of individual nucleated seed of magnetic Ni and induce its growth along the direction of lines of magnetic force. Fig. 3b shows the SEM image of S1m. It is mainly composed of rodlike crystallite with diameter around 380 nm and length over 2 μm and some agglomerated particles with smaller size, consistent with the preferential orientation growth result analyzed by the XRD data. In order to further investigate the composition changes induced by the magnetic field, the energy dispersive spectroscopy (EDS) was conducted for sample S1m. Curves a and b in Fig. 3c are EDS ones for boxed area and circled area in Fig. 3b. The ratios of Ni to Cu are 67:33 and 39:61 for boxed area and circled one, respectively. Clearly, the rodlike products in boxed area are Ni-rich phase, while spherical products in circled area are Cu-rich particles.

Fig. 4 shows the SEM images of S2 and S2m. Compared with the morphological change of sample S1m, the introduction of magnetic field exerts less influence on S2m. Sample S2 possesses spherical morphology, while S2m is less spherical or quasi-spherical. Both the size of S2m (on average, 400 nm) and its size distribution are larger than those of S2 (on average, 60 nm). The higher dosage of PVP is clearly helpful to the formation of spherical particles and reduction of particles size. With the increase of PVP dosage, the adsorption probability of PVP long chain molecules for Cu^{2+} and Ni^{2+} are enhanced, which would limit the growth of Ni crystallite and counteract the magnetic field induction effect, and should be responsible for the observation that the morphological changes are not as obvious as those changes of S1m.

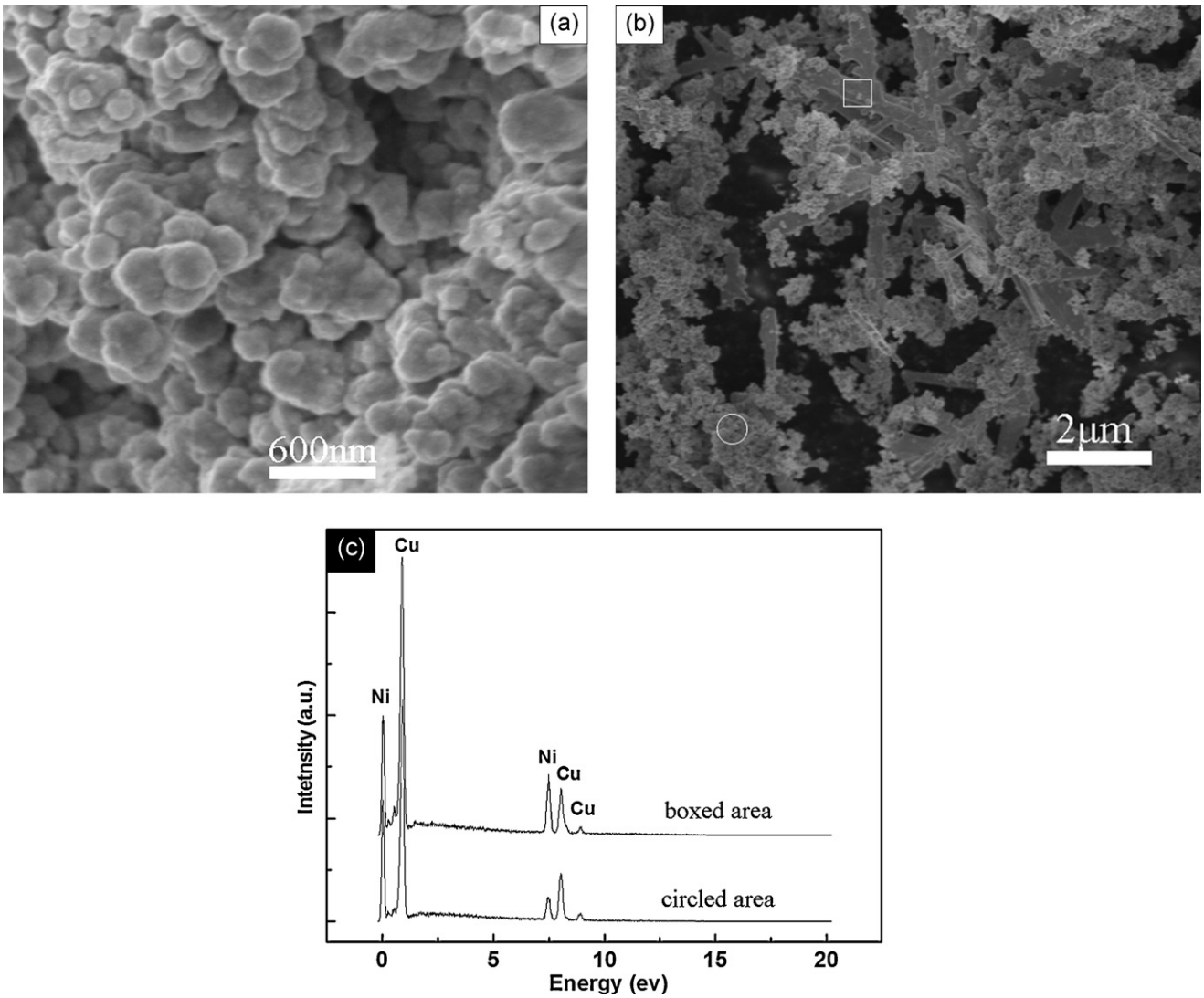

Fig. 3. SEM images of samples S1 and S1m. (a) S1, (b) S1m, (c) EDX patterns for circled area and boxed area in (b).

Moreover, considering the magnetic property difference between crystalline Ni (ferromagnetic) and Cu (diamagnetic), it is naturally understood that S2m possesses a bigger size distribution than that of S2 and the distorted spherical shape of S2m. The synergistic roles played by PVP dosage and magnetic field induction effect should be responsible for all these morphological observations.

The magnetic properties of materials are believed to be highly dependent on the sample morphology, crystalline, magnetization direction, etc. [21]. Hence, the ferromagnetic properties of S1m and S2m are supposed to be remarkably different from those of S1 and S2. Fig. 5 shows *M*–*H* hysteresis loops of the products measured at room temperature. The inset is the enlarged plots of boxed area in Fig. 5. The main magnetic parameters including saturation magnetization M_s, remnant magnetization M_r, reduced magnetization M_r/M_s and coercive field H_c are listed in Table 1. Two behaviors can be distinguished:

(1) The induction of magnetic field could result in the increase of magnetic parameters. For example, Sample S1 and S2 possessed saturation magnetization of 27.2 and 13.0 emu/g, both of which are lower than that of 31.1 and 16.8 emu/g for S1m and S2m, respectively. This phenomenon of increase in M_s holds for other three parameters. The explanation of improved magnetic properties for samples S1m and S2m can be analogous to our previous reports of NiCo alloys and magnetite chainlike microstructures [17,22]. In the presence of the magnetic field, the diffusion rate Ni^{2+}, and Cu^{2+} in the solution is increased and this diffusion rate increase will favor the nucleation and growth of particles, improve the crystallinity and hence enhance the saturation magnetization. Interestingly, magnetic field exerts much more distinct effect on S1m than on S2m in terms of M_r, and reduced magnetization M_r/M_s.

(2) The choice of PVP dosage could be used to control particles size. Compared with S1, sample S2 possesses much smaller size. In

Table 1
Magnetic parameters M_s, M_r, M_r/M_s, H_c of S1, S1m, S2, S2m measured by VSM at room temperature.

Samples	Parameters			
	M_s (emu/g)	M_r (emu/g)	M_r/M_s	H_c (Oe)
S1	27.1	3.2	0.12	106
S1m	31.1	11.2	0.36	156
S2	13.0	4.5	0.34	195
S2m	16.8	5.7	0.34	234

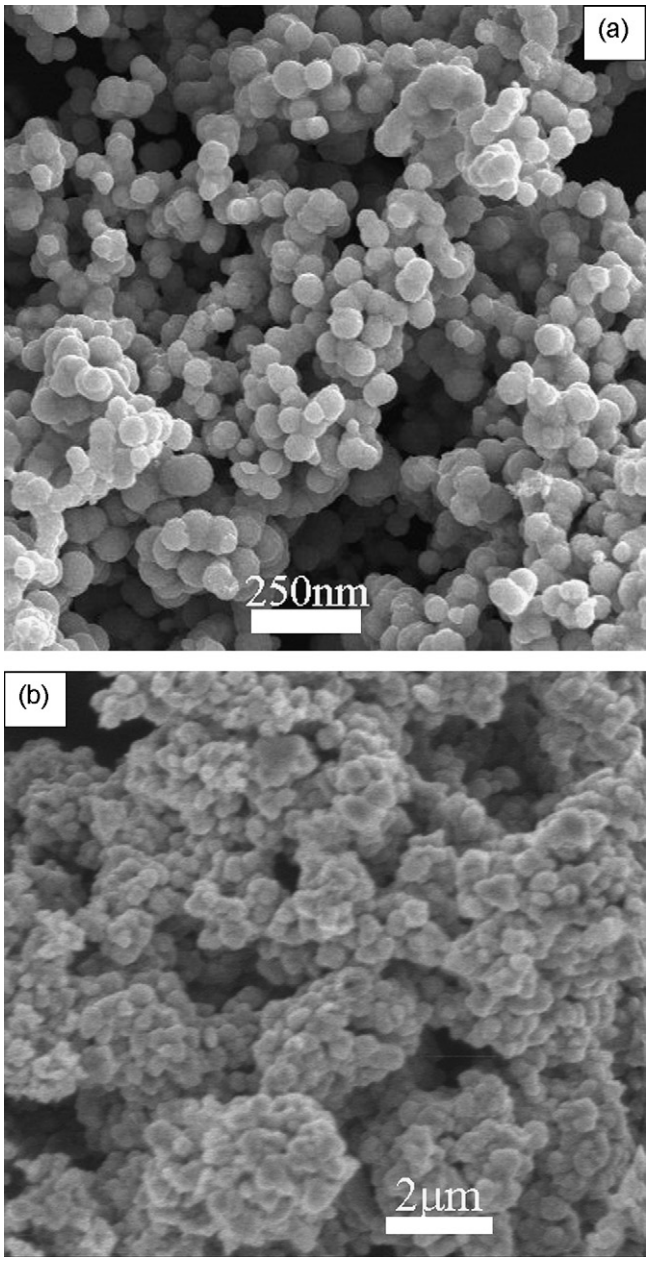

Fig. 4. SEM images of samples S2 and S2m. (a) S2, (b) S2m.

the presence of higher dosage of PVP, PVP molecules are abundant in the solution for the coating of the nucleated particles' surfaces and prevent the particles from growing. The smaller the particles size is, the worse the crystallinity is, the thicker the dead layer of the particles would be, and the smaller magnetic parameters should be.

On the basis of the criteria given by Dunlop [23], single-domain (SD) particles have a value of M_r/M_s larger than 0.5, pseudo-single-domain (PSD) particles have a value between 0.1 and 0.5 and multidomain (MD) particles have a value lower than 0.1. From Table 1, all of these four samples possess a PSD-type behavior. The changes of M_r/M_s values imply that the application of magnetic field could exert much influence on the magnetic domain. Although all of these four samples are of PSD-type domain, the great changes of M_r/M_s for S1 and S1m and magnetic properties changes of these four samples imply that the magnetic field

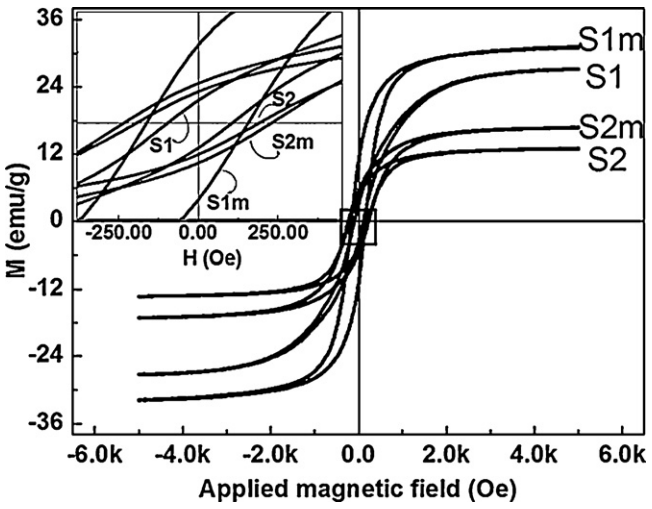

Fig. 5. Field-dependent magnetization of samples S1, S1m, S2, S2m measured at 300 K in an applied magnetic field of up to 10,000 Oe. The inset shows the enlarged plots in boxed area.

plays a role in the nucleation, growth and domain control of particles.

4. Conclusions

In summary, an interesting case of magnetic field-induced changes in products' morphology, composition and magnetic properties are reported, which indicates that the magnetic field could play an important role in the nucleation, growth and domain control of particles. Therefore, the application of magnetic field is supposed to be an important tool to control the composition, morphology and properties of magnetic materials.

Acknowledgements

This work was supported by National Natural Science Foundation of China (50901074, 50672001), Anhui Provincial Natural Science Fund (070414202), and Young Teacher Natural Science Fund of Anhui Province (2008jq1002).

References

[1] Q.A. Pankhurst, R.J. Pollard, Phys. Rev. Lett. 67 (1991) 248.
[2] F. Levy, I. Sheikin, B. Grenier, A.D. Huxley, Science 309 (2005) 1343.
[3] C.T. Rodgers, P.J. Hore, Proc. Natl. Acad. Sci. 106 (2009) 353.
[4] K. Maeda, A.J. Robinson, K.B. Henbest, E.J. Dell, C.R. Timmel, J. Am. Chem. Soc. 132 (2010) 1466.
[5] X. Commeinhes, P. Davidson, C. Bourgaux, J. Livage, Adv. Mater. 9 (1997) 900.
[6] J. Wang, Q.W. Chen, C. Zeng, B.Y. Hou, Adv. Mater. 16 (2004) 137.
[7] P. Beecher, E.V. Shevchenko, H. Weller, A.J. Quinn, G. Redmond, Adv. Mater. 17 (2005) 1080.
[8] D.S. Lu, W.S. Li, X. Jiang, C.L. Tan, R.H. Zeng, J. Alloys Compd. 485 (2009) 621.
[9] R.M. Erb, H.S. Son, B. Samanta, V.M. Rotello, B.B. Yellen, Nature 457 (2009) 999.
[10] T. Ozdemir, D. Sandal, M. Culha, A. Sanyal, N.Z. Atay, S. Bucak, Nanotechnology 21 (2010) 125603.
[11] U. Wiedwald, M. Cerchez, M. Farle, K. Fauth, G. Schütz, K. Zürn, H.G. Boyen, P. Ziemann, Phys. Rev. B 70 (2004) 214412.
[12] T. Kimura, Y. Sato, F. Kimura, M. Iwasaka, S. Ueno, Langmuir 21 (2005) 830.
[13] T. Liu, Q. Wang, A. Gao, C. Zhang, D.G. Li, J.C. He, J. Alloys Compd. 481 (2009) 755.
[14] S. Tao, J.J. Tian, X. Lu, X.H. Qu, Y. Honkura, H. Mitarai, K. Noguchi, J. Alloys Compd. 477 (2009) 510.
[15] X.S. Fang, Y. Bando, U.K. Gautam, C.H. Ye, D. Golbergkjlk, J. Mater. Chem. 18 (2008) 509.
[16] L.D. Zhang, X.S. Fang, J. Nanosci. Nanotechnol. 8 (2008) 149.
[17] M.Z. Wu, G.Q. Liu, M.T. Li, P. Dai, Y.Q. Ma, L.D. Zhang, J. Alloys Compd. 491 (2010) 689.
[18] H.Q. Sun, Y.N. Shi, J. Mater. Sci. Technol. 25 (2009) 347.

[19] J.W.T. Heemskerk, Y. Noat, D.J. Bakker, J.M.V. Ruitenbeek, B.J. Thijsse, P. Klaver, Phys. Rev. B 67 (2003) 115416.
[20] J. Toth, E. Toth-Kadar, A. Dinia, V. Pierron-Bohnes, I. Bakonyi, L.F. Kiss, J. Magn. Magn. Mater. 198/199 (1999) 243.
[21] Z.P. Liu, S. Li, Y. Yang, S. Peng, Z.K. Hu, Y.T. Qian, Adv. Mater. 15 (2003) 1946.
[22] M.Z. Wu, Y. Xiong, Y.S. Jia, H.L. Niu, H.P. Qi, J. Ye, Q.W. Chen, Chem. Phys. Lett. 40 (2005) 374.
[23] R.M. Cornell, U. Schwertmann, The Iron Oxides: Structure, Properties, Reactions, Occurrences and Uses, Wiley-VCH Verlag GmbH & Co. KgaA, Weinheim, Germany, 2003, p. 141.